# Tryptophan Fluorescence of Terminal Deoxynucleotidyl Transferase: Effects of Quenchers on Time-Resolved Emission Spectra†

David J. Robbins, Martin R. Deibel, Jr.,‡ and Mary D. Barkley*
*Department of Biochemistry, University of Kentucky Medical Center, Lexington, Kentucky 40536-0084*
*Received December 27, 1984*

ABSTRACT: Terminal deoxynucleotidyl transferase (EC 2.7.7.31) is a eucaryotic DNA polymerase that does not require a template. The tryptophan environments in calf thymus terminal transferase were investigated by fluorescence. The heterogeneous emission from this multitryptophan enzyme was separated by time-resolved emission spectroscopy. Nanosecond fluorescence decays at 296-nm excitation and various emission wavelengths were deconvolved by global analysis, assuming that the lifetimes but not the relative weighting factors were independent of emission wavelength. The data were fit to three exponentials of lifetimes $\tau_1$ = 1.4 ns, $\tau_2$ = 4.5 ns, and $\tau_3$ = 7.7 ns. The corresponding decay-associated emission spectra of the three components had maxima at about 328, 335, and 345 nm. The accessibility of individual tryptophan environments to polar and nonpolar fluorescence quenchers was examined in steady-state and time-resolved experiments. In the presence of iodide and acrylamide, the steady-state emission spectra shift to the blue. However, at low quencher concentrations, the emission from the 7.7-ns component (maximum 345 nm) is hardly affected, suggesting that this hydrophilic tryptophan environment is buried within the protein. On the other hand, the red shift in the steady-state emission spectrum in the presence of trichloroethanol indicates that the 1.4-ns component (maximum 328 nm) is an exposed hydrophobic tryptophan environment. The results are consistent with an inside-out model for terminal transferase protein, with the more hydrophobic tryptophan(s) near the surface and the most hydrophilic tryptophan(s) in the core.

Terminal deoxynucleotidyl transferase synthesizes single-stranded DNA in vitro by 5′ to 3′ addition of deoxynucleoside triphosphates to a primer. It is unique among known DNA polymerases in that it does not require a template. This property of the enzyme is exploited commercially to synthesize DNA of defined base composition and to end-label DNA molecules for programmed recombinational events. Terminal transferase is expressed only in mammalian or avian thymic and bone marrow prelymphocytes and the neoplastic counterparts of these cells. Clinical interest in terminal transferase arose from the observation that certain types of leukemic cells express elevated levels of terminal transferase activity (McCaffrey et al., 1973; Coleman et al., 1974). A number of studies have correlated terminal transferase activity with leukemia subtype and disease state (Greenwood et al., 1977; Coleman & Hutton, 1981). Although the in vivo role of terminal transferase is still unknown, the enzyme activity is a marker for primitive lymphoid cells (Deibel et al., 1983).

Detailed biochemical studies have been conducted with calf thymus terminal transferase. Although the original molecular weight of the purified enzyme was determined to be 32 000 (Chang & Bollum, 1971), a modified purification procedure produced a larger ($M_r$ 44 000) protein (Deibel & Coleman, 1980a). Since then, higher molecular weight forms have been detected by immunochemical screening, and degradation schemes have been proposed (Chang et al., 1982; Deibel et al., 1983). The highest known molecular weight form of the calf thymus enzyme ($M_r$ 58 000) has been purified (Chang et al., 1982). So far, no differences in catalytic properties have been found between the higher and lower molecular weight forms. Kinetic studies of terminal transferase isolated from calf thymus (Kato et al., 1967) and human lymphoblasts (Deibel & Coleman, 1980b) have been presented [see also Coleman & Deibel (1983) for review]. Terminal transferase was shown to exhibit a random sequential mechanism, allowing it to bind either substrate independent of the other. Physical and chemical studies have been hampered by difficulties in isolating and handling terminal transferase and by its resistance to chemical modification. Thus, intrinsic tryptophan fluorescence offers an attractive method for investigating such a protein. Because tryptophan emission is sensitive to solvent polarity, information concerning the local environments of tryptophan residues may be revealed. In addition, the effects of collisional quenchers on the emission indicate the degree of solvent accessibility of the tryptophans.

Calf thymus terminal transferase was initially reported to contain three tryptophan residues: two in the $\beta$ subunit and one in the $\alpha$ subunit (Chang & Bollum, 1971). More recent data from nucleotide sequencing of a cloned gene for human terminal transferase (Peterson et al., 1984) and from amino acid sequencing of calf thymus terminal transferase (Peterson et al., 1984; Beach et al., 1985) show at least two tryptophans in the $\alpha$ subunit, as well as at least two more in the $\beta$ subunit. Since proteins with a single tryptophan residue usually exhibit multiple fluorescence lifetimes (Grinvald & Steinberg, 1976; Beechem & Brand, 1985), the emission of multitryptophan proteins such as terminal transferase is expected to be complex. Recently, computer algorithms have been developed to deal with complex fluorescence decay data and to separate the spectra of individual fluorescent components (Ross et al., 1981; Knutson et al., 1982). The method employed in this work simultaneously deconvolutes fluorescence decay data from a given sample taken at different wavelengths. In general, if some parameters can be assumed constant in several data sets, a global analysis of these data may be performed to over-

† This work was supported by NIH Grants GM 31076 and GM 22873. D.J.R. was the recipient of USPHS National Research Service Award CA-07542 from the National Cancer Institute.
* Address correspondence to this author at the Department of Chemistry, Louisiana State University, Baton Rouge, LA 70803-1804.
‡ Present address: Biopolymer Chemistry, Upjohn Co., Kalamazoo, MI 49001.

0006-2960/85/0424-7250$01.50/0 © 1985 American Chemical Society

determine the remaining variables (Knutson et al., 1983). The global analysis used here requires no prior knowledge of the fluorescence lifetimes but does assume them to be constant across the emission spectrum. If the total emission spectrum of a protein can be separated into its constitutive components, then the individual tryptophan environments can be examined in quenching studies by steady-state (Eftink & Ghiron, 1981) and time-resolved fluorescence methods (Ross et al., 1981).

In this paper we present fluorescence studies of terminal transferase, which to our knowledge are the first such studies of a eucaryotic DNA polymerase. We combine the results of steady-state quenching experiments and of fluorescence lifetime measurements in the absence and presence of quenchers to elucidate the environment of the tryptophan residues in the enzyme. After decomposing the steady-state emission spectrum into emission spectra from three temporally distinct sources, we deduce from the effects of quenchers that the protein consists of a hydrophobic exterior around a hydrophilic interior.

## Experimental Procedures

### *Materials*

*N*-Acetyl amides of tryptophan and tyrosine were purchased from Sigma Chemial Co. (St. Louis, MO). Reagent-grade acrylamide was recrystallized from ethyl acetate. Ethylene glycol (99+%) and trichloroethanol were from Aldrich Chemical Co. (Milwaukee, WI). All other chemicals were reagent-grade.

### *Methods*

*Enzyme Purification and Assay.* Terminal deoxynucleotidyl transferase was isolated from calf thymus by the method of Chang & Bollum (1971), with the modifications introduced by Deibel & Coleman (1980). Following oligo(dT)–cellulose chromatography, a protein was obtained with a native $M_r$ of 44000 and two nonidentical subunits $\alpha$ ($M_r$ 12000) and $\beta$ ($M_r$ 32000) in a 1:1 stoichiometry. Protein concentrations were determined by the Lowry assay (Lowry et al., 1951). On the basis of these data and an assumed $M_r$ of 44000 (Deibel & Coleman, 1980) an extinction coefficient of approximately 35000 $M^{-1}$ $cm^{-1}$ at 275 nm was determined. The specific activity of preparations used in this work was 100000 units/mg or greater. Protein was routinely stored in 25 mM potassium phosphate buffer, pH 7.4, containing 50% glycerol at −20 °C.

Enzyme activity was assayed as previously described (Deibel & Coleman, 1980) with $p(dA)_{50}$ and [$^3$H]dATP as substrates. In order to examine the effects of fluorescence quenchers on enzyme activity, the assay was also performed in the presence of acrylamide or KI. Terminal transferase retained 95% and 77% of its activity in the presence of 0.5 and 1 M acrylamide, respectively. The residual activities of terminal transferase in the presence of the same concentrations of KI were 11% and 1%, respectively. Inactivation of enzyme by KI is presumably due to the salt-dependent reduction in the binding constant for $p(dA)_{50}$.

*Steady-State Fluorescence Measurements.* All steady-state fluorescence measurements were performed in a SPEX Fluorolog 211 controlled by a Datamate terminal. The spectrofluorometer was operated in the ratio mode. Glans polarizers oriented at 0 and 55° were used to correct for anisotropic effects. The temperature of the sample was maintained at 10 °C. Excitation was at 296 nm; protein absorbance at this wavelength was less than 0.1 with a 4-mm path length. Emission spectra (29-nm band-pass) were corrected for wavelength-dependent instrument response.

Three classes of quenchers were used: ionic ($I^-$), polar nonionic (acrylamide), and nonpolar (trichloroethanol). The resulting shifts of emission maxima and the amount of quenching as a function of wavelength and quencher concentration were recorded either by scanning the tryptophan emission band (300–400 nm) or by measuring quenching at 315, 337, and 370 nm. Small aliquots from freshly prepared 1, 2, or 8 M stock solutions of acrylamide or KI (containing sodium thiosulfate to retard $I_3^-$ formation) or from a 1 M stock solution of trichloroethanol in ethylene glycol were added to a 2 $\mu$M solution of terminal transferase in 25 mM potassium phosphate, pH 7.2. Fluorescence intensities were corrected for additional absorbance by acrylamide at 296 nm (Lakowicz, 1983). With a path length of 4 mm and an extinction coefficient of $\epsilon_{296} = 0.25$ $M^{-1}$ $cm^{-1}$, the correction amounted to 1.23 times the observed fluorescence in the presence of 1 M acrylamide. Additions of trichloroethanol were performed with care, following the suggestions of Eftink et al. (1977). Emission at 450 nm was also monitored for evidence of any photochemical reaction of trichloroethanol with terminal transferase.

*Lifetime Measurements.* Fluorescence lifetimes were measured in a Photochemical Research Associates nanosecond fluorometer equipped with a Tracor Northern TN-1750 multichannel analyzer with 2K memory. The flash lamp was operated at 30 kHz, with 5 kV applied across a 1.5-mm electrode gap under 1.7 atm of $N_2$. The lamp pulse width was 1.4–1.6 ns fwhm. Excitation wavelength was selected through a 10-nm band-pass interference filter with 26% transmission at 296 nm (microCoatings, Westford, MA). Since the excitation light is virtually unpolarized, emission was viewed through a single polarizer rotated to 35° on the emission side. A 2-mm slit (16-nm band-pass) was used for the emission monochromator. Samples were thermostated at 10 °C, and cuvettes were defogged by a stream of nitrogen. Data acquisition was controlled by a Digital Equipment Corp. MINC-11 computer.

Protein samples contained 10 $\mu$M terminal transferase (absorbance approximately 0.1 at 296 nm with a 4-mm path length) in 25 mM potassium phosphate, pH 7.2; the glycerol content of these solutions was approximately 9%. Fluorescence decay data were collected by alternating among a Ludox solution (to measure instrumental response), a protein sample, a buffer blank, and a monoexponential standard ($10^{-4}$ M *N*-acetyltryptophanamide in 0.1 M sodium phosphate, pH 7.2). The sample dwell time was 5 min/cycle; the experiment was continued until the sample decay curve contained approximately 10000 counts in the peak. A complete experiment consisted of lifetime measurements at five to seven emission wavelengths between 310 and 393 nm in the absence and presence of 30 mM acrylamide or 50 mM KI and 500 mM quencher. Such a set of measurements took approximately 4 days of counting. At the end of the experiment, however, the UV spectrum of the protein showed no evidence of denaturation.

If the fluorescence decay $I(\lambda,t)$ is assumed to be a sum of exponentials, then

$$I(\lambda,t) = \sum_i \alpha_i(\lambda) \exp(-t/\tau_i) \quad (1)$$

where $\alpha_i(\lambda)$ is the preexponential weighting factor at emission wavelength $\lambda$ and $\tau_i$ is the fluorescence lifetime for the $i$th component. This model assumes that the lifetimes are independent of wavelength and only the weighting factors change across the emission band. The fluorescence decay from the *N*-acetyltryptophanamide standard acquired concurrently was

deconvolved to determine the wavelength-dependent time shift in the instrumental response function for each sample decay. A global analysis program was then employed to deconvolve the fluorescence decays collected at different emission wavelengths simultaneously for each concentration of quencher. The global program uses a nonlinear least-squares method to fit the data (Bevington, 1969). Goodness of fit was evaluated from the reduced $\chi_r^2$, and the quality of fit was judged by the autocorrelation function of the weighted residuals (Grinvald & Steinberg, 1974).

If the decays at each wavelength were acquired for the same time and the lamp intensity did not fluctuate, the preexponential weighting factor $\alpha_i(\lambda)$ would be the emission envelope and the product $\alpha_i(\lambda)\tau_i$ the steady-state intensity of each component. In practice, however, the steady-state intensities of the components were obtained by scaling the $\alpha_i(\lambda)$'s to the steady-state spectrum. For each wavelength $\lambda$ examined in the nanosecond fluorometer, the corresponding steady-state intensity $I(\lambda)$ must be the sum of the intensities from each lifetime component. The intensity $I_i(\lambda)$ due to component $i$ is given by

$$I_i(\lambda) = I(\lambda)\frac{\alpha_i(\lambda)\tau_i}{\sum_i \alpha_i(\lambda)\tau_i} \quad (2)$$

*Measurement of Tryptophan Content.* Chang & Bollum (1971) reported that the $M_r$ 32000 calf thymus terminal transferase contained three tryptophans, as measured by ultraviolet absorption. In order to compare this result with our larger protein ($M_r$ 44000), we measured the tyrosine/tryptophan ratio in 6 M guanidine hydrochloride by using the second derivative of the UV spectrum (Servillo et al., 1982). According to recent amino acid analysis data of M. S. Coleman (personal communication), the $\alpha$ and $\beta$ subunits of terminal transferase contain 12 tyrosine residues. The average of eight determinations yielded a ratio of 2.5 ± 0.3 tyrosine residues per tryptophan, which implies four to five tryptophans in the $M_r$ 44000 protein. All absorbance measurements were performed on a Cary 118C spectrophotometer.

## Results

*Steady-State Quenching.* Tryptophan emission is sensitive to solvent polarity. The fluorescence emission maximum of tryptophan in water occurs at 348 nm (Teale & Weber, 1957), compared to 300 nm in hexane (Lakowicz, 1983). Emission maxima at shorter (blue) wavelengths indicate a less polar environment, while maxima at longer (red) wavelengths indicate a more polar environment. If the total emission spectrum is composed of heterogeneous emission spectra, then the susceptibility of different components to fluorescence quenchers will be a function of their relative accessibility. Thus, spectral shifts observed upon addition of quenchers would indicate the existence of more than one tryptophan environment. Figure 1 compares the emission spectrum of terminal transferase (emission maximum at 337 nm) to that in the presence of 1 M polar nonionic (acrylamide) or 300 mM nonpolar (trichloroethanol) quenchers. At high concentrations, acrylamide shifts the terminal transferase spectrum to shorter wavelengths by 10 nm. The effects of KI were similar but less dramatic, producing a blue shift of 7 nm. In contrast, at low concentrations of trichloroethanol, the entire emission spectrum is uniformly quenched. As the trichloroethanol concentration exceeds 150 mM, the emission peak is shifted to longer wavelengths by about 10 nm.

Stern–Volmer plots of fluorescence quenching data in the blue (315-nm) and red (370-nm) portions of the terminal

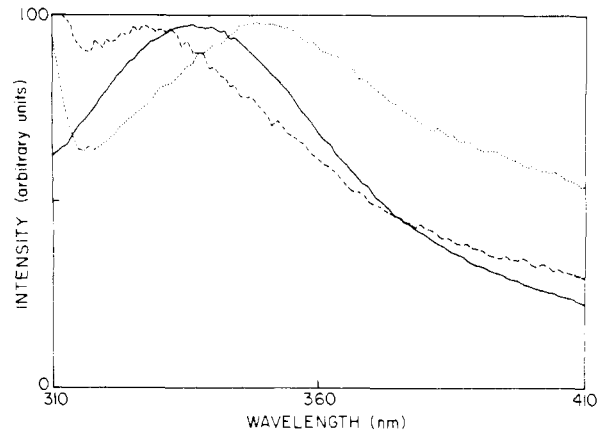


FIGURE 1: Steady-state emission spectra of terminal transferase in the absence and presence of quenchers: (—) no quencher, $\lambda_{em}^{max}$ = 337 nm; (– –) 1 M acrylamide, $\lambda_{em}^{max}$ = 327 nm; (···) 0.3 M trichloroethanol, $\lambda_{em}^{max}$ = 348 nm. Samples were excited at 296 nm (14-nm band-pass). The spectra were normalized at their peaks.

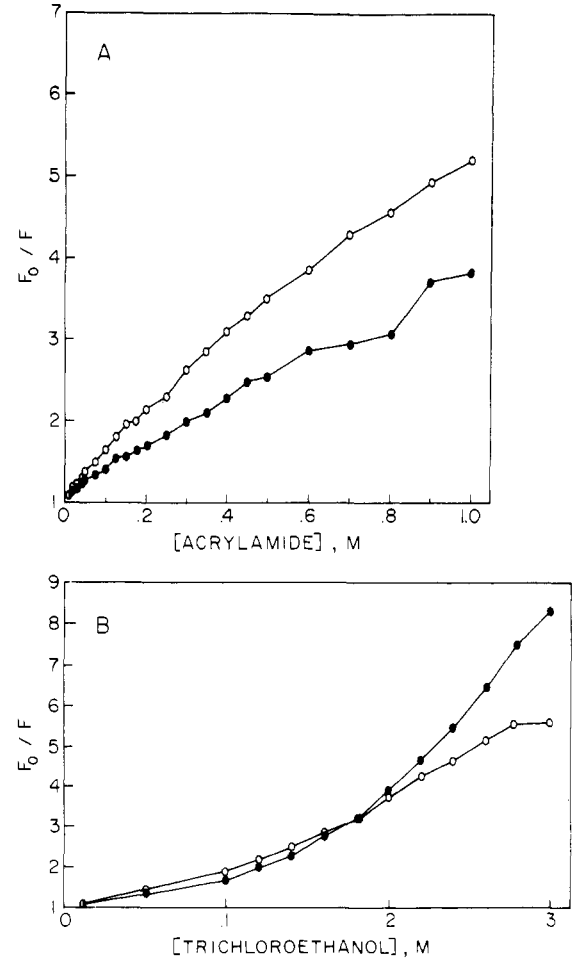


FIGURE 2: Stern–Volmer plots of terminal transferase quenched by (A) acrylamide or (B) trichloroethanol. Intensity at (●) 315 and (○) 370 nm.

transferase emission spectrum are presented in Figure 2 for acrylamide and trichloroethanol. These plots as well as the modified Stern–Volmer plots (not shown) are not linear but are useful for qualitative comparison of quencher efficiency in different regions of the emission band. For the case of one accessible emitter and one inaccessible emitter, a linear modified plot of $F_0/\Delta F$ vs. $1/[Q]$ would have an intercept of $1/f_a$ and a slope of $1/(f_a K_{sv})$ (Lehrer, 1971), where $f_a$ is the fraction of tryptophan emission accessible to quencher and $K_{sv}$

Table I: Fluorescence Quenching Data from Modified Stern–Volmer Plots

| concn (mM) | quencher | $\lambda_{em}$ (nm) | $f_a$[a] | $K_{sv}$(eff) ($M^{-1}$)[b] |
|---|---|---|---|---|
| 20–75 | KI | 315 | 0.10 | 58 |
| | | 337 | 0.09 | 63 |
| | | 370 | 0.12 | 31 |
| | acrylamide | 315 | 0.39 | 21 |
| | | 337 | 0.44 | 28 |
| | | 370 | 0.51 | 22 |
| 20–80 | trichloroethanol | 315 | 0.95 | 22 |
| | | 337 | 1.00 | 20 |
| | | 370 | 0.86 | 27 |
| 350–700 | KI | 315 | 0.76 | 1.8 |
| | | 337 | 0.78 | 1.9 |
| | | 370 | 0.83 | 1.3 |
| | acrylamide | 315 | 0.92 | 3.9 |
| | | 337 | 1.00 | 4.9 |
| | | 370 | 0.94 | 6.4 |

[a] Fraction of total tryptophan emission accessible by quencher. [b] Effective Stern–Volmer quenching constant (Eftink & Ghiron, 1981).

is the Stern–Volmer quenching constant for the accessible emission. The slope of the initial linear portion of the Stern–Volmer plot (commonly taken as $K_{sv}$) will be equal to the product $f_a K_{sv}$ determined from the slope of the modified plot. In the case of multiple emitting species, the general expression for the modified plot is

$$F_0/\Delta F = [\sum_i f_i K_{svi}[Q]/(1 + K_{svi}[Q])]^{-1} \quad (3)$$

where $f_i$ [$=\alpha_i\tau_i/(\sum\alpha_i\tau_i)$] is the fractional intensity and $K_{svi}$ is the Stern–Volmer constant of component $i$. For low quencher concentrations, the curve becomes linear with an intercept of $\sum f_i K_{svi}^2/(\sum f_i K_{svi})^2$ and a slope of $1/(\sum f_i K_{svi})$. The parameters obtained from the Lehrer plot therefore contain contributions from all of the emitting species. Table I compares results from the approximately linear regions of the modified plots for all three quenchers employed. Since the $f_a$'s and $K_{sv}$(eff)'s are effective quenching parameters, one can look only at general trends across the emission spectrum and from quencher to quencher. The trends in $f_a$ as a function of quencher type and concentration provide insight into the various tryptophan environments that give rise to emission in different portions of the spectrum. At low concentrations of quencher, ionic iodide affected only about 10% of the total tryptophan emission but with the highest $K_{sv}$(eff). Acrylamide influenced 40–50% of the total emission with a high $K_{sv}$(eff). For example, the mean lifetime, $\langle\tau\rangle$ ($=\sum f_i\tau_i$), calculated from the data in Table II is 6.3 ns at 370-nm emission. The mean Stern–Volmer constant, $\langle K_{sv}\rangle$ ($=\sum f_i K_{svi}$), obtained from the product of $f_a$ and $K_{sv}$(eff) in Table I is 11 $M^{-1}$ at this wavelength. Taking $\langle K_{sv}\rangle$ to be approximately equal to $k_q\langle\tau\rangle$, we estimate an effective bimolecular quenching constant of about $1.7 \times 10^9$ $M^{-1}$ $s^{-1}$. This value is within the range expected for accessible tryptophan residues in proteins (Eftink & Ghiron, 1981). In contrast to these hydrophilic quenchers, most of the emission was accessible to trichloroethanol with approximately the same $K_{sv}$(eff) as observed for acrylamide. Thus, for low concentrations of quenchers, terminal transferase tryptophans are more accessible to hydrophobic than to hydrophilic quenchers. At high quencher concentrations, almost all of the emission was accessible to acrylamide while still only about 80% was accessible to iodide. On the other hand, the $K_{sv}$(eff)'s for these two quenchers were greatly reduced compared to the $K_{sv}$(eff)'s observed at lower quencher concentrations. Thus, the tryptophan(s) readily quenched by iodide is (are) probably a surface residue(s) in a hydrophilic environment (Lehrer, 1971). As indicated by Figure 2, higher concentrations of trichloroethanol induced enhanced levels of quenching of the 315-nm portion of the spectrum compared to the 370-nm portion. Trichloroethanol could not be introduced in concentrations greater than 300 mM without causing protein precipitation, as commonly observed (Eftink et al., 1977). Protein also precipitated at trichloroethanol concentrations of 30–50 mM in the more concentrated terminal transferase solutions used for time-resolved experiments.

Table II: Fluorescence Decay Parameters for Nine Emission Wavelengths[a]

| $\lambda_{em}$ (nm) | $\alpha_1(\lambda)$ | $\alpha_2(\lambda)$ | $\alpha_3(\lambda)$ |
|---|---|---|---|
| 320 | 0.47 ± 0.01 | 0.43 ± 0.02 | 0.10 ± 0.01 |
| 328 | 0.39 ± 0.05 | 0.43 ± 0.02 | 0.16 ± 0.03 |
| 335 | 0.35 ± 0.05 | 0.45 ± 0.06 | 0.20 ± 0.02 |
| 340 | 0.36 ± 0.09 | 0.41 ± 0.04 | 0.23 ± 0.05 |
| 345 | 0.27 ± 0.07 | 0.47 ± 0.08 | 0.27 ± 0.03 |
| 355 | 0.22 ± 0.07 | 0.47 ± 0.09 | 0.32 ± 0.04 |
| 365 | 0.18 ± 0.04 | 0.45 ± 0.06 | 0.37 ± 0.05 |
| 370 | 0.17 ± 0.06 | 0.42 ± 0.02 | 0.41 ± 0.06 |
| 375 | 0.12 ± 0.10 | 0.45 ± 0.10 | 0.43 ± 0.06 |
| $\tau_i$ (ns) | 1.4 ± 0.3 | 4.5 ± 0.3 | 7.7 ± 0.5 |

[a] Results of global analysis of time-resolved emission spectral data. Lifetimes are mean values for six experiments. Relative preexponential factors $\alpha_i(\lambda)$ are mean values for two to four experiments; $\sum\alpha_i(\lambda) = 1$. Errors are standard deviations.

The spectral shifts observed in the presence of quenchers provide evidence for multiple emission sources with different emission spectra. Therefore, we attempted to separate the overlapping spectra by time-resolved emission spectroscopy.

*Time-Resolved Emission Spectra of Terminal Transferase.* In order to determine the number of components necessary to describe the terminal transferase tryptophan emission, fluorescence decay data were deconvolved by single-curve analysis of decays at each wavelength and by global analysis of decays from several emission wavelengths. Theoretical fits were generated for two- and three-exponential models. Figure 3 is an example of the results for 335-nm emission comparing (A) a two-exponential fit obtained by single-curve analysis of the data at that wavelength ($\chi_r^2 = 1.9$) and (B) a three-exponential fit generated by a global analysis of data from five emission wavelengths (individual $\chi_r^2 = 1.6$, global $\chi_r^2 = 1.3$). Also attempted were a three-exponential fit by single-curve analysis ($\chi_r^2 = 1.6$; $\alpha_1 = 0.38$, $\tau_1 = 1.3$ ns, $\alpha_2 = 0.44$, $\tau_2 = 4.6$ ns, $\alpha_3 = 0.18$, $\tau_3 = 7.7$ ns) and a two-exponential fit generated by global analysis (individual $\chi_r^2 = 2.3$, global $\chi_r^2 = 1.5$; $\alpha_1 = 0.59$, $\tau_1 = 2.3$ ns, $\alpha_2 = 0.41$, $\tau_2 = 6.8$ ns). In comparison, the *N*-acetyltryptophanamide standard was fit with a single-exponential decay of 3.3 ns ($\chi_r^2 = 1.1$). The global $\chi_r^2$ is the sum of the $\chi_r^2$ for the individual decay curves in the global fit divided by the number of curves used in the analysis. For the experiment in Figure 3, the global $\chi_r^2$ for a three-exponential decay was 1.3; the individual $\chi_r^2$ of the other four curves (not shown) ranged from 1.1 to 1.3 by both single-curve and global analyses. These same data were fit by a two-exponential decay with a global $\chi_r^2$ of 1.5 and individual $\chi_r^2$ values ranging from 1.2 to 2.3. Since the improvement in $\chi_r^2$ for a three-exponential fit compared to a two-exponential fit was not very large, the choice of three exponentials was made by inspection of the autocorrelation functions. All attempts to fit terminal transferase data to two-exponential decays resulted in autocorrelation functions deviating systematically from zero (Figure 3A). However, these data could be fit to three-exponential decays by single-curve or global analysis with autocorrelation functions fluctuating around zero (Figure 3B). The autocorrelation functions for the monoexponential standard also fluctuated

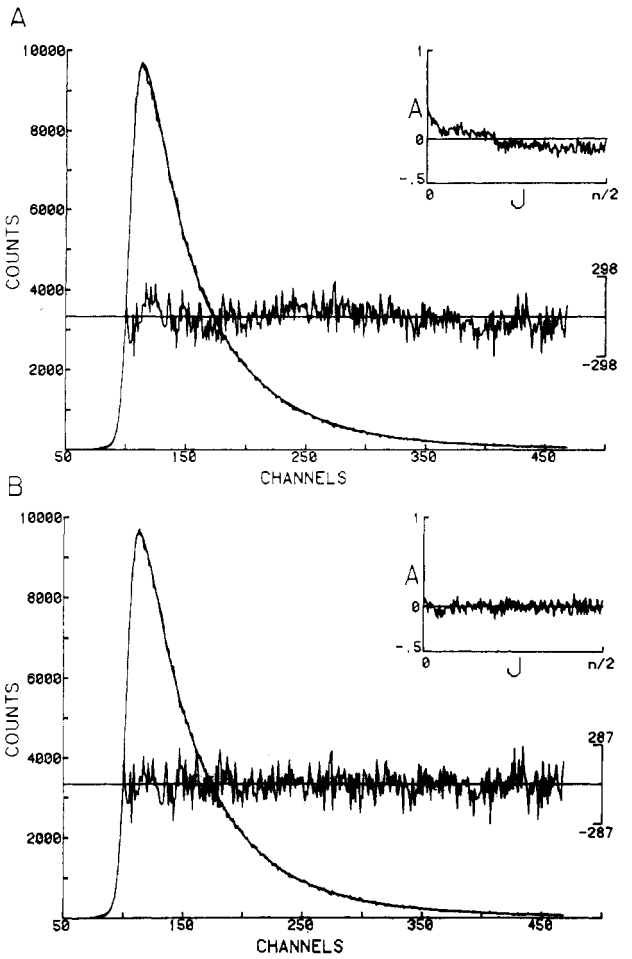


FIGURE 3: Fluorescence decay of terminal transferase. Timing calibration 0.109 ns/channel, $\lambda_{ex}$ = 296 nm, and $\lambda_{em}$ = 335 nm. The data were fit to (A) two exponentials by single-curve analysis ($\chi_r^2$ = 1.9, $\alpha_1$ = 0.51, $\tau_1$ = 1.8 ns, $\alpha_2$ = 0.49, $\tau_2$ = 6.3 ns) and (B) three exponentials by a global analysis of decay curves at five emission wavelengths (335–375 nm in 10-nm intervals) ($\chi_r^2$ = 1.6, $\alpha_1$ = 0.36, $\tau_1$ = 1.3 ns, $\alpha_2$ = 0.42, $\tau_2$ = 4.3 ns, $\alpha_3$ = 0.22, and $\tau_3$ = 7.5 ns). The percent residuals and autocorrelation functions (inset) are also shown.

around zero (not shown), indicating that there were no systematic instrumental errors. The choice of three exponentials over two exponentials is further supported by the tryptophan content of the protein. Because terminal transferase has at least four tryptophan residues, we expect at least four exponential decays (Beechem & Brand, 1985), but it is unlikely that we could resolve them all. On the basis of the $\chi_r^2$ and autocorrelation functions, it was concluded that three exponentials adequately described the data. Although single curve analysis will find the best parameters for any one curve, only the global analysis will determine the best parameter set consistent with all the available data.

As noted under Methods, the preexponential factors $\alpha_i(\lambda)$ from the time-resolved emission spectrum are required to construct the decay-associated spectra, which represent the contributions of individual components to the steady-state spectrum. Table II gives the preexponential weighting factors for various wavelengths, along with the three lifetimes. Here, the $\alpha_i(\lambda)$'s for each emission wavelength were normalized to unity. Figure 4 presents the steady-state spectrum of terminal transferase and the decay-associated spectra of the three-exponential components, which were constructed according to eq 2 from the values in Table II. For those wavelengths at which more than one experiment was performed, the error bars indicate the propagated errors computed from the standard

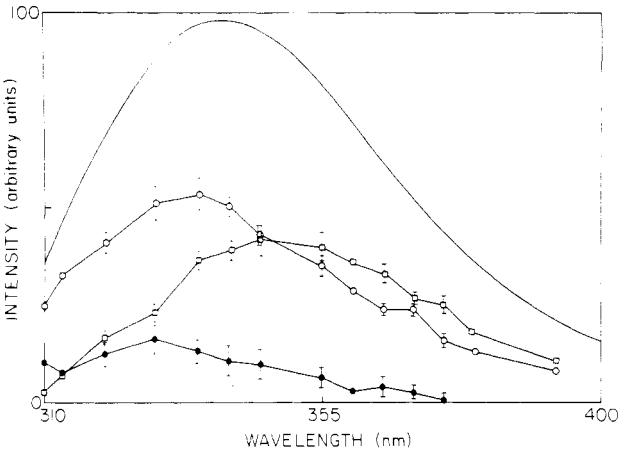


FIGURE 4: Decay-associated emission spectra of terminal transferase. (Upper curve) Steady-state spectrum, excitation at 296 nm (3.6-nm band-pass). Steady-state contributions from (●) component 1, $\tau_1$ = 1.4 ns, (○) component 2, $\tau_2$ = 4.5 ns, and (□) component 3, $\tau_3$ = 7.7 ns. Spectra were constructed from decay parameters given in Table II and in one other experiment. Error bars are propagated errors from Table II.

deviations listed in Table II. With excitation at 296 nm, the emission maxima for the three components associated with $\tau_1$ = 1.4 ns, $\tau_2$ = 4.5 ns, and $\tau_3$ = 7.7 ns decays were about 328, 335, and 345 nm, respectively. Thus, component 1 reports on a relatively nonpolar environment and component 3 a polar environment, while component 2 reflects an intermediate case.

*Effects of Quenchers on Individual Time-Resolved Emission Spectra of Terminal Transferase.* Since the emission spectrum of terminal transferase could be resolved into three temporally distinct environments, the next step was to seek a connection between the decay-associated spectra and the steady-state spectral shifts observed upon addition of quenchers. If a single tryptophan residue (or several residues in the same environment) gives rise to two of the constructed spectra, then the response of these spectra to addition of quencher should be uniform. If, however, each tryptophan environment is associated with only one spectrum, then the response of each spectrum to added quencher will be different. It is also possible that one or more of the three observed lifetimes represent several unresolved lifetimes. If the unresolved components differ in their susceptibility to quenching, then three exponential decays may no longer fit the data. Alternatively, the emission from one or more of the unresolved components, which contributed to one decay-associated spectrum in the unquenched protein, may in the presence of quencher be averaged into a different decay-associated spectrum. This would be evidenced by distinct decreases in some $\alpha_i(\lambda)$'s and increases in other $\alpha_j(\lambda)$'s coupled with shifts of the affected decay-associated spectra as quencher is added. These possibilities were examined by constructing the decay-associated spectra of quenched terminal transferase and comparing the quenching patterns of individual spectra to the corresponding spectra from unquenched protein.

After fluorescence lifetime measurements were made on a sample of terminal transferase, the steady-state emission spectrum was measured before and after addition of a low (30 mM acrylamide or 50 mM KI) quencher concentration. After correction for dilution, these spectra are a direct measure of steady-state quenching for the sample. A new set of lifetime measurements was then made. This pattern of steady-state spectra before and after quencher addition followed by lifetime measurements was repeated for a high (0.5 M) quencher concentration. Table III presents the values of $\tau_i$ for terminal

Table III: Decay Parameters in the Presence of Acrylamide[a]

| acrylamide concn | $\alpha_1(345)$ | $\tau_1$ (ns) | $\alpha_2(345)$ | $\tau_2$ (ns) | $\alpha_3(345)$ | $\tau_3$ (ns) |
|---|---|---|---|---|---|---|
| 0[b] | 0.27 ± 0.07 | 1.4 ± 0.3 | 0.47 ± 0.08 | 4.5 ± 0.3 | 0.27 ± 0.03 | 7.7 ± 0.5 |
| 30 mM[c] | 0.19 ± 0.01 | 1.2 ± 0.4 | 0.36 ± 0.08 | 3.7 ± 0.6 | 0.31 ± 0.01 | 6.5 ± 0.5 |
| 0.5 M[c] | 0.26 ± 0.04 | 1.0 ± 0.1 | 0.31 ± 0.05 | 2.4 ± 0.1 | 0.09 ± 0.01 | 5.1 ± 0.1 |

[a] Results of global analysis of time-resolved emission spectra data. [b] Values taken from Table II; $\sum\alpha_i(345) = 1$. [c] Mean values for three experiments. Preexponential factors are for emission at 345 nm and are scaled to the relative steady-state intensities.

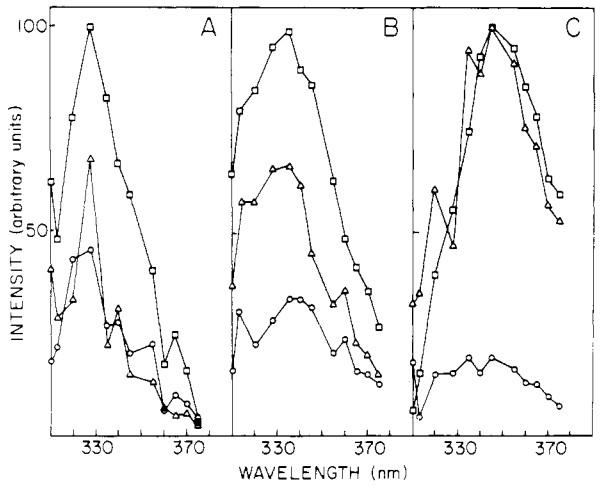


FIGURE 5: Effects of quencher on decay-associated emission spectra of terminal transferase. Results for (A) component 1, (B) component 2, and (C) component 3. (□) Spectra from Figure 4 in the absence of quencher normalized to the peak for each component. (△) 30 mM acrylamide: $\tau_1 = 1.2 \pm 0.4$ ns, $\tau_2 = 3.7 \pm 0.6$ ns, and $\tau_3 = 6.5 \pm 0.5$ ns. (○) 0.5 M acrylamide: $\tau_1 = 1.0 \pm 0.1$ ns, $\tau_2 = 2.4 \pm 0.1$ ns, and $\tau_3 = 5.1 \pm 0.1$ ns. Intensities for each component in the presence of quencher are relative to unquenched component.

transferase in the absence and presence of 30 mM and 0.5 M acrylamide as well as values of $\alpha_i$ for 345-nm emission. For each quencher concentration, a new set of decay-associated emission spectra were constructed, which showed the quenching patterns of the three lifetimes separated previously. Figure 5 shows the decay-associated emission spectra from terminal transferase as a function of acrylamide concentration. The quenching patterns observed for iodide were similar. In Figure 2, the steady-state spectrum was shifted to the blue upon addition of iodide or acrylamide. Figure 4 indicates that the contributions of components 2 and 3 to the steady-state intensity of terminal transferase are approximately equal. For low acrylamide concentration, Figure 5 shows that the observed blue shift is associated primarily with quenching of component 2. Thus, although component 3 describes the most polar environment of the protein, it was not the most accessible to iodide or acrylamide. At 0.5 M acrylamide, component 3 was highly quenched.

According to Figure 5, each decay-associated spectrum had a unique quenching pattern upon addition of acrylamide. In the presence of 30 mM acrylamide, the decrease in the lifetime of component 1 agrees within experimental error with the decrease in the decay-associated spectrum (Figure 5A). The lifetime of component 2 is not quenched quite as much as its decay-associated spectrum (Figure 5B). The small decreases in some of the $\alpha_2(\lambda)$'s, however, are within the error of measurement. The lifetime of component 3 decreases slightly more than the error, while its decay-associated spectrum does not change significantly (Figure 5C). The compensating increases in the $\alpha_3(\lambda)$'s are again, however, within the error of measurement. The quenching patterns observed for 50 mM iodide were similar, differing only in that iodide quenching of components 2 and 3 was not as efficient. However, here the decreases in lifetimes and decay-associated spectra were equal within experimental error. Given the standard deviations of Table II, no consistent pattern of changes in the $\alpha_i(\lambda)$'s of any component was detected for either acrylamide or iodide quenching at low quencher concentrations. Therefore, we conclude that the observed quenching is primarily dynamic (Eftink & Ghiron, 1981).

In the presence of 0.5 M acrylamide, no systematic change in the values of the $\alpha_1(\lambda)$'s are seen. On the other hand, the decay-associated spectra of components 2 and 3 are quenched more than the lifetimes. The observed decrease in the $\alpha_3(\lambda)$'s with no corresponding increase in the other $\alpha_i(\lambda)$'s indicates that the intensity is removed by static quenching rather than transferred from component 3 to another component. Smaller decreases in the $\alpha_2(\lambda)$'s are also noted, leaving the assignment of static quenching a possible but not necessary explanation. On the other hand, static quenching is not evident in the presence of 0.5 M iodide. The lifetime of component 2 is quenched to about the same extent as the decay-associated spectrum. The spectrum of component 1 is approximately equal to the unquenched spectrum although the lifetime is quenched by 20%. The $\alpha_3(\lambda)$'s decrease systematically but less than in the case of acrylamide. Since this decrease in the $\alpha_3(\lambda)$'s is accompanied by a corresponding increase in the $\alpha_1(\lambda)$'s, it appears that emission from a tryptophan(s) contributing to component 3 becomes associated with component 1 in the presence of high concentrations of iodide. All observed quenching by iodide can thus be explained without invoking static quenching. The behavior of component 3 in the presence of high quencher concentrations indicates that it consists of at least two species, one of which can be statically quenched by acrylamide or sufficiently quenched by iodide so that its lifetime becomes inseparable from that of component 1. Since a two-exponential decay will not fit these data, part of component 3 must persist with only a moderately quenched (34% in 0.5 M acrylamide; 18% in 0.5 M iodide) lifetime and thus be highly resistant to any quenching process.

With an emission maximum at about 345 nm, the decay-associated spectrum of component 3 must decribe a relatively hydrophilic (polar) region. Low concentrations of quenchers did not affect the spectrum, indicating that this hydrophilic region is not readily accessible to solvent. The decay-associated spectrum of component 1, with an emission maximum at approximately 328 nm, decribes a hydrophobic region that was accessible by nonionic polar (acrylamide) quencher but not by ionic (iodide) quencher. This region thus must be close enough to the protein surface to allow access by acrylamide but hydrophobic enough to resist quenching by iodide. The comparatively low concentration of quenchers needed to quench the decay-associated spectrum of component 2 (emission maximum at about 335 nm) suggests a relatively hydrophilic exposed region.

## DISCUSSION

In order to determine the nature of the local tryptophan environments of terminal transferase, results from both

steady-state and time-resolved fluorescence experiments were combined. Since terminal transferase is a multitryptophan enzyme, the first step was to determine whether the emission was heterogeneous. The shifts in the emission maximum observed upon addition of fluorescence quenchers indicate that the spectrum must be composed of at least two different spectra. Quenching by ionic (iodide) or nonionic polar (acrylamide) quenchers progressively shifted the emission maximum to the blue, indicating that the longer wavelength emission is due to an accessible hydrophilic region. Low concentrations of the organic hydrophobic quencher trichloroethanol affected the entire emission spectrum uniformly, but concentrations greater than 150 mM predominantly quenched the blue portion of the spectrum. Trichloroethanol has been shown to sense hydrophobic regions of proteins and cluster in these areas, leading to exaggerated quenching (Eftink et al., 1977). The quenching pattern at 315 nm in Figure 2 resembles that for human serum albumin [Figure 2 of Eftink et al. (1977)]. These observations indicate that there are distinct hydrophilic and hydrophobic tryptophan environments on terminal transferase.

The heterogeneous emission revealed in steady-state experiments implies that the steady-state spectrum may be separated into a number of distinct emissions, each with a characteristic spectrum and fluorescence lifetime. The total fluorescence decay of terminal transferase was measured at several wavelengths across the emission band. These data were analyzed according to a multiexponential model with lifetimes independent of wavelength but weighting factors that depend on emission wavelength. On the basis of the $\chi_r^2$ and autocorrelation function, it was concluded that a three-exponential decay adequately describes the data.

Because multiexponential decays have been observed from proteins containing only a single tryptophan (Grinvald & Steinberg, 1976), further evidence was sought to show that the three components separated from the total terminal transferase emission spectrum represented different tryptophan environments. The susceptibility of the individual components to quenchers was examined by fluorescence lifetime measurements to see if the three components had unique quenching patterns and, if so, to what extent the patterns explain the steady-state quenching results. According to Table I, the fraction of accessible tryptophan emission was slightly greater at 370 nm than at 315 nm. Figure 4 reveals, however, that the three components have overlapping emission spectra so the steady-state parameters will not be well resolved. The quenching patterns shown in Figure 5 indicate that although component 3 reflects a hydrophilic environment, it is *not* readily accessible by quenchers at low concentration. Since the steady-state observations indicated quenching at 370 nm, this must be due mostly or entirely to quenching of component 2. For example, at 30 mM acrylamide, we found 27% steady-state quenching at 370 nm. At 370 nm, component 3 was quenched only 10% while component 2 was quenched 45% (Figure 5). Comparison of the steady-state contributions of these two components (neglecting the contribution from component 1) yields 25% steady-state quenching.

The results for acrylamide and iodide quenching indicate that the three spectral components may be associated with tryptophan environments with the following characteristics: component 2 emanates from a hydrophilic surface residue readily accessible by iodide and acrylamide; component 3 is a more hydrophilic region (emission maximum at longer wavelength) that is not readily accessible to either iodide or acrylamide, indicating its location within the protected terminal transferase interior; component 1 is a hydrophobic region that must be close to the protein surface due to its accessibility by acrylamide. Since iodide does not appear to quench component 1 effectively, it must be in a very hydrophobic pocket. Further evidence of this is the enhanced quenching observed by addition of trichloroethanol.

The tyrosine/tryptophan ratio of terminal transferase was found to be 2.5 by the method of Servillo et al. (1982). This indicated that there are four to five tryptophans per $M_r$ 44000 protein (12 tyrosine residues; M. S. Coleman, personal communication). Recent nucleotide sequence data from a cDNA clone of human terminal transferase (Peterson et al., 1984) and amino acid sequence data from calf thymus terminal transferase (Peterson et al., 1984; Beach et al., 1985) show one probable and two definite tryptophans in the smaller $\alpha$ subunit and at least two definite tryptophans in the larger $\beta$ subunit. Although the entire amino acid sequence of the calf enzyme has not been determined, it is clear that there must be more tryptophan residues than temporally distinct lifetime components. Within the 10-nm spectral resolution of our time-resolved experiments, the results presented here agree with a terminal transferase model in which one or more of the lifetime components represent the approximately homogeneous emission of more than one tryptophan. How many tryptophans comprise each decay-associated spectrum and specific assignments of these spectra to locations on the enzyme are future questions that can be dealt with in a manner similar to our present approach. The effects on tryptophan emission of polydeoxynucleotide or deoxynucleoside triphosphate substrate binding may indicate which spectral region corresponds to the tryptophans close to the active site of the enzyme. Further progress toward assignments may be possible if the subunits of terminal transferase can be separated in a nondenatured form or if native forms of the protein with one or more tryptophans deleted can be isolated by selective limited proteolysis. Of interest is comparison of the present results to those from enzymatically active higher molecular weight forms of terminal transferase.

## ACKNOWLEDGMENTS

We thank Joseph M. Beechem and Prof. Ludwig Brand for helpful discussions about global analysis. We are grateful to Dr. Zbigniew Kolber and Dorota Gmerck for writing a global program for the MINC-11 computer.

**Registry No.** $I^-$, 20461-54-5; $Cl_3CCH_2OH$, 115-20-8; acrylamide, 79-06-1; L-tryptophan, 73-22-3; terminal deoxynucleotidyl transferase, 9027-67-2.

## REFERENCES

Beach, C. M., Vanaman, T. C., Chan, S. K., & Coleman, M. S. (1985) *Biochem J. 227*, 1003–1007.

Beechem, J. M., & Brand, L. (1985) *Annu. Rev. Biochem. 54*, 43–71.

Bevington, P. R. (1969) *Data Reduction and Error Analysis for the Physical Sciences*, McGraw-Hill, New York.

Chang, L. M. S., & Bollum, F. J. (1971) *J. Biol. Chem. 246*, 909–916.

Chang, L. M. S., Plevani, P., & Bollum, F. J. (1982) *J. Biol. Chem. 257*, 5700–5706.

Coleman, M. S., & Deibel, M. R. (1983) in *Enzymes of Nucleic Acid Synthesis and Modification* (Jacob, S. T., Ed.) Vol. I, pp 93–118, CRC Press, Boca Raton, FL.

Coleman, M. S., Hutton, J. J., DeSimone, P., & Bollum, F. J. (1974) *Proc. Natl. Acad. Sci. U.S.A. 71*, 4404–4408.

Deibel, M. R., & Coleman, M. S. (1980a) *Arch. Biochem. Biophys. 202*, 414–419.

Deibel, M. R., & Coleman, M. S. (1980b) *J. Biol. Chem. 255*, 4206–4212.
Deibel, M. R., Riley, L. K., & Coleman, M. S. (1983) *Isozymes: Curr. Top. Biol. Med. Res. 7*, 297–315.
Eftink, M. R., & Ghiron, C. A. (1981) *Anal. Biochem. 114*, 199–227.
Eftink, M. R., Zajicek, J. L., & Ghiron, C. A. (1977) *Biochim. Biophys. Acta 491*, 473–481.
Greenwood, M. F., Coleman, M. S., Hutton, J. J., Lampkin, B., Krill, C., Bollum, F. J., & Holland, P. (1977) *J. Clin. Invest. 59*, 889–899.
Grinvald, A., & Steinberg, I. Z. (1974) *Anal. Biochem. 59*, 583–598.
Grinvald, A., & Steinberg, I. Z. (1976) *Biochim. Biophys. Acta 427*, 663–678.
Kato, K.-I., Goncalves, J. M., Houts, G. E., & Bollum, F. J. (1967) *J. Biol. Chem. 242*, 2780–2789.
Knutson, J. R., Walbridge, D. G., & Brand, L. (1982) *Biochemistry 21*, 4671–4679.
Knutson, J. R., Beechem, J. M., & Brand, L. (1983) *Chem. Phys. Lett. 102*, 501–507.
Lakowicz, J. R. (1983) *Principles of Fluorescence Spectroscopy*, p 44, Plenum, New York.
Lakowicz, J. R., & Cherek, H. (1980) *J. Biol. Chem. 255*, 831–834.
Lehrer, S. S. (1971) *Biochemistry 10*, 3254–3263.
Lowry, O. H., Rosebrough, N. J., Farr, A. L., & Randall, R. J. (1951) *J. Biol. Chem. 193*, 265–275.
McCaffrey, R., Smoler, D. F., & Baltimore, D. (1973) *Proc. Natl. Acad. Sci. U.S.A. 70*, 521–525.
Peterson, R. C., Cheung, L. C., Mattaliano, R. J., Chang, L. M. S., & Bollum, F. J. (1984) *Proc. Natl. Acad. Sci. U.S.A. 81*, 4363–4367.
Ross, J. B. A., Schmidt, C. J., & Brand, L. (1981) *Biochemistry 20*, 4369–4377.
Servillo, L., Colonna, G., Balestrieri, C., Ragone, R., & Irace, G. (1982) *Anal. Biochem. 126*, 251–257.
Teale, F. W. J., & Weber, G. (1957) *Biochem. J. 65*, 476–482.

# Structural Elucidation of a Hydrophobic Box in Bovine α-Lactalbumin by NMR: Nuclear Overhauser Effects†

Keiko Koga and Lawrence J. Berliner*
*Department of Chemistry, The Ohio State University, Columbus, Ohio 43210*
*Received April 26, 1985*

ABSTRACT: The proton nuclear Overhauser effects of bovine α-lactalbumin were studied at 200 MHz by irradiation of an upfield ring current shifted methylene at −2.45 ppm (assigned to Ile-95) and two aromatic protons, Tyr-103 (8.36 ppm) and Trp-60 (5.85 ppm). The experimental results were consistent with a putative three-dimensional α-lactalbumin model [Warme, P. K., Momany, F. A., Rumball, S. V., Tuttle, R. W., & Scheraga, H. A. (1974) *Biochemistry 13*, 768–782], which predicted the close proximity of Ile-95, Tyr-103, Trp-60, and Trp-104. Several of the assignments correlated with those previously made from chemically induced dynamic nuclear polarization experiments [Berliner, L. J., & Kaptein, R. (1981) *Biochemistry 20*, 799–807]. Subtle differences in the structure of this hydrophobic box region in α-lactalbumin were found between the Ca(II) and apo forms of the protein. The existence of this "hydrophobic box" in α-lactalbumin was strikingly similar to that in lysozyme, as verified *in solution*.

α-Lactalbumin (α-LA)[1] is a modifier protein in the lactose synthase complex whose function is to modify the acceptor specificity of galactosyl transferase from GlcNAc to glucose. The molecular details of the interaction between α-LA and galactosyl transferase still remain unclear, nor has an X-ray structure of α-LA been reported to date. However, an energy-minimized, three-dimensional structure was described by Warme et al. (1974) based on primary sequence homologies to hen egg white (HEW) lysozyme. It is desirable to test the validity of this putative model *in solution* by experiments that may elucidate detailed molecular structural features. The nuclear Overhauser effect (NOE) is an extremely powerful method for investigating the tertiary structure of proteins *in solution* [for example, see Keller & Wüthrich (1981)]. The NOE reflects specific dipolar interactions between nuclei, which are distance-dependent and thus provide information about the relative positions of an irradiated, saturated nucleus and those nuclei that experience a change in intensity as a result of this initial irradiation (Noggle & Schirmer, 1971). Recently, Poulsen et al. (1980) verified the existence of a "hydrophobic box" in HEW lysozyme by $^1$H NMR NOE measurements, consistent with its X-ray structure.

It has recently been shown that α-LA is a calcium binding protein (Hiroaka et al., 1980) that undergoes a distinct conformational change upon cation binding (Permyakov et al., 1981a,b; Murakami et al, 1982). In this work, we show by NOE measurements the existence of a hydrophobic box structure in bovine α-LA that is remarkably similar to that of HEW lysozyme. Furthermore, we note some subtle dif-

† This work was supported in part by Grant HD 17270 from the USPHS. The 200-MHz NMR instrument used in these studies was funded by NIH Grant GM 27431 to L.J.B. (co-PI) for core research.

[1] Abbreviations: α-LA, α-lactalbumin; GlcNAc, *N*-acetylglucosamine; HEW, hen egg white; NOE, nuclear Overhauser effect; Tris-DCl, tris(hydroxymethyl)aminomethane-$d_{11}$; FT, Fourier transform.; FID, free induction decay; DSS, sodium 2,2-dimethyl-2-silapentane-5-sulfonate; CIDNP, chemically induced dynamic nuclear polarization; 1D, one dimensional.

0006-2960/85/0424-7257$01.50/0 © 1985 American Chemical Society